

## Triplet $s$ -wave resonance in ${}^6\text{Li}$ collisions and scattering lengths of ${}^6\text{Li}$ and ${}^7\text{Li}$

E. R. I. Abraham, W. I. McAlexander, J. M. Gerton, and R. G. Hulet  
*Physics Department and Rice Quantum Institute, Rice University, Houston, Texas 77251-1892*

R. Côté and A. Dalgarno  
*Harvard-Smithsonian Center for Astrophysics, 60 Garden Street, Cambridge, Massachusetts 02138*  
 (Received 13 January 1997)

The triplet  $s$ -wave scattering length of  ${}^6\text{Li}$  is determined using two-photon photoassociative spectroscopy of the diatomic  $a\ ^3\Sigma_u^+$  state of  ${}^6\text{Li}_2$ . The measured binding energy of the highest-lying bound state, combined with knowledge of the potential, determines the  $s$ -wave scattering length to be  $(-2160 \pm 250)a_0$ , where  $a_0$  is the Bohr radius. This extraordinarily large scattering length signifies a near-threshold resonance. A complete table of singlet and triplet scattering lengths for collisions involving  ${}^6\text{Li}$  and  ${}^7\text{Li}$  determined from this and our previous spectroscopic investigations is given.

[S1050-2947(97)50605-6]

PACS number(s): 34.20.Cf, 33.20.Fb, 32.80.Pj

The recent achievement of Bose-Einstein condensation (BEC) in atomic gases [1] has enabled new opportunities for the investigation of quantum-statistical effects in dilute gases. Although dilute, interactions are vitally important in the formation, dynamics, and stability of the gas. In these experiments, the densities are sufficiently low that usually only two-body interactions are important, and the temperatures low enough that elastic interactions can be described by a single parameter, the  $s$ -wave scattering length  $a$  [2]. The magnitude of  $a$  is a measure of the strength of the interaction and its sign indicates whether the interaction is effectively repulsive ( $a > 0$ ) or attractive ( $a < 0$ ). In the case of a bosonic atom, such as  ${}^7\text{Li}$ , a negative scattering length can prevent BEC in a homogeneous gas [3] and limit the number of condensed atoms for a trapped gas [4], as was recently observed [5]. For a fermionic atom, such as  ${}^6\text{Li}$ , a large and negative scattering length may enable the observation of a BCS-like phase transition [6].

Accurate knowledge of the two-body interaction potential is necessary to calculate  $a$ . Two ground-state alkali-metal atoms interact via electronic spin-singlet  $X\ ^1\Sigma_g^+$  and spin-triplet  $a\ ^3\Sigma_u^+$  molecular potentials, with scattering lengths  $a_S$  and  $a_T$ , respectively. While  $a$  is a function of the entire interaction potential, it is most sensitive to the binding energy of the least-bound vibrational level [7]. The extreme case of a state lying very near the dissociation limit produces a zero-energy scattering resonance. When a potential gives a state that is only weakly bound,  $a$  is large and positive, while a slightly shallower potential in which the state is not bound produces a large and negative value.

Since lithium occurs naturally with stable bosonic and fermionic isotopes, it is particularly well suited to studies of degenerate quantum gases. In a series of studies [7–10], we have used photoassociative spectroscopy to sensitively probe the interaction potentials of both isotopes. For the triplet potential, we used two-photon photoassociative spectroscopy to measure directly the binding energy of the least-bound state of  ${}^7\text{Li}_2$ , which gave  $a_T$  to high precision [7]. This scattering length, which is the relevant one for the doubly spin-

polarized gas used in the  ${}^7\text{Li}$  BEC experiments of Refs. [1] and [5], is unambiguously negative. In this paper, we report the results of a similar two-photon measurement of the triplet state of  ${}^6\text{Li}_2$  and show that there is a near-threshold resonance that produces a negative scattering length of extraordinary magnitude. Since the spectroscopy is now complete, we give a comprehensive table of all singlet and triplet scattering lengths for both isotopes as well as for a mixed isotope gas using improved values for the long-range interaction coefficients [11].

A discussion of the experimental apparatus and procedure is given elsewhere [8]. A photoassociating laser beam of frequency  $\omega_P$  is passed through a cloud of  ${}^6\text{Li}$  atoms that are confined in a magneto-optical trap (MOT). When  $\omega_P$  is resonant with the unbound state of two colliding atoms and a bound excited molecular state, the two atoms can be promoted to the excited state. The excited molecular state can spontaneously decay to a bound, ground-state molecule that is untrapped, or to two free atoms that may have sufficient kinetic energy to escape the trap. Both mechanisms lead to a reduction in the total number of atoms in the trap that is observed using a photodiode as a decrease in the trap laser-induced fluorescence.

Two-photon photoassociative spectroscopy [7] is illustrated schematically in Fig. 1. Another independently tunable laser beam of frequency  $\omega_B$  is overlapped with the photoassociation laser beam in the region of the trapped atoms and is tuned to be resonant with the bound excited state and the highest-lying bound state of the ground-state molecular potential. This second laser reduces the population of the excited state, and an increase in the trap laser-induced fluorescence occurs as fewer atoms are lost via spontaneous emission, as discussed in Ref. [7]. Figure 2(a) shows an experimental signal for one-photon photoassociation; the two-photon signal for the  ${}^6\text{Li}$  transition depicted in Fig. 1, obtained by fixing  $\omega_P$  and scanning  $\omega_B$ , is shown in Fig. 2(b). A theoretical treatment of two-photon photoassociative spectroscopy, including the line shape, was presented in Ref. [12].

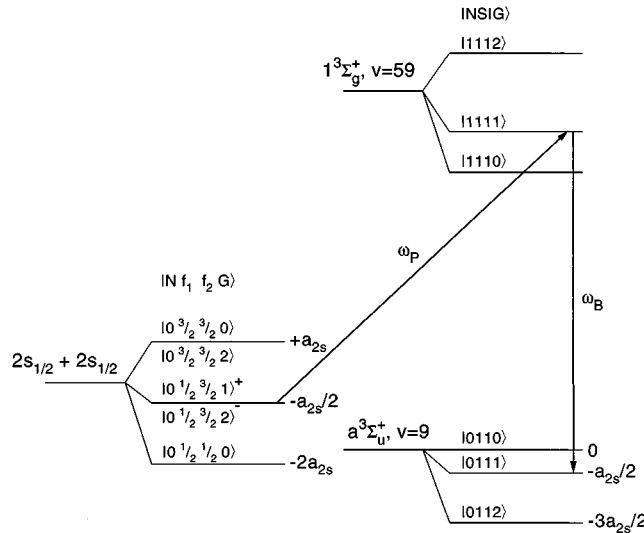


FIG. 1. Energy-level diagram of the two-photon photoassociation of the  $v=9$ ,  $N=0$  level of the  $a^3\Sigma_u^+$  state of  ${}^6\text{Li}_2$ . For the initial free state the relevant quantum numbers  $|Nf_1f_2G\rangle$  are indicated and the energies are relative to the hyperfine center of gravity, where  $a_{2s}$  is the atomic  $2s_{1/2}$  hyperfine constant. The notation  $|Nf_1f_2G\rangle^\pm$  identifies a superposition of two states given by  $2^{-1/2}(|Nf_1f_2G\rangle \pm |Nf_2f_1G\rangle)$ , which occurs when  $f_1 \neq f_2$ . For the intermediate state  $1^3\Sigma_g^+$ , hyperfine levels  $|NSIG\rangle$  are shown for  $N=1$ . For the final state  $a^3\Sigma_u^+$ , the hyperfine energies of the levels  $|NSIG\rangle$  are given for  $N=0$  relative to their hyperfine center of gravity.

The two-photon process involves an initial state of two free atoms, an excited intermediate molecular state, and a final molecular ground state. In the initial state, each colliding  ${}^6\text{Li}$  atom has nuclear spin  $i=1$  and electronic spin  $s=1/2$ , and can be in either hyperfine state  $f=1/2$  or  $f=3/2$ , where  $\vec{f}=\vec{s}+\vec{i}$  is the total atomic angular momentum. There are three possible hyperfine energies, corresponding to both atoms in  $f=1/2$ , both atoms in  $f=3/2$ , or one atom in each hyperfine level. The energy shift of the initial state relative to the  $2s_{1/2}+2s_{1/2}$  hyperfine center of gravity is

$$E_{Nf_1f_2G} = \frac{a_{2s}}{2} \left[ f_1(f_1+1) + f_2(f_2+1) - \frac{11}{2} \right], \quad (1)$$

where  $a_{2s}$  is the atomic  $2s_{1/2}$  hyperfine constant. Because of the ultralow temperatures in the MOT ( $\sim 1$  mK), the collisions are predominantly  $s$ -wave, with the rotational angular momentum  $N=0$ . The total spin angular momentum is  $\vec{G}=\vec{f}_1+\vec{f}_2$ . The initial energy is independent of  $\vec{G}$  due to the weak coupling between  $\vec{f}_1$  and  $\vec{f}_2$ . Since the  ${}^6\text{Li}$  atom is a composite fermion, only certain values of  $G$  are allowed, due to the requirement that the total wave function be antisymmetric with respect to exchange of identical atoms. A complete description of the allowed states and symmetries is given in Ref. [10], and the possible initial states are depicted in Fig. 1.

The  $v=59$ ,  $N=1$   $1^3\Sigma_g^+$  excited molecular state was used as the intermediate level. Since this level is well described by Hund's case (b) coupling [10], the total electronic spin,  $\vec{S}=\vec{s}_1+\vec{s}_2$ , and the total nuclear spin,  $\vec{I}=\vec{i}_1+\vec{i}_2$ , are good

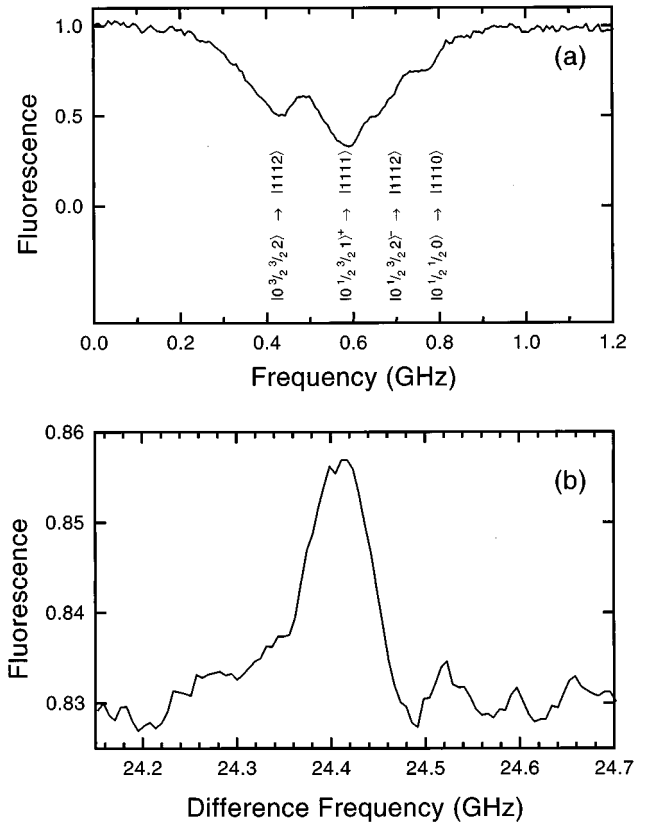


FIG. 2. (a) One-photon photoassociation of the  $v=59$ ,  $N=1$  vibrational level of the  $1^3\Sigma_g^+$  state of  ${}^6\text{Li}_2$ . The trap laser-induced fluorescence, scaled to its value in the absence of photoassociation, is plotted vs  $\omega_p$ . The initial- and intermediate-state quantum numbers of the states involved in the transitions are indicated by the notation  $|Nf_1f_2G\rangle \rightarrow |NSIG\rangle$ , as in Fig. 1. One allowed transition,  $|0\frac{3}{2}\frac{3}{2}1\rangle \rightarrow |11110\rangle$ , is not resolved. The  $v=59$ ,  $N=1$  vibrational level has a binding energy of 1787 GHz and an outer turning point of  $35a_0$ . (b) Two-photon photoassociation of the  $v=9$ ,  $N=0$  vibrational level of the  $a^3\Sigma_u^+$  state of  ${}^6\text{Li}_2$ . The quantum numbers for the final state are  $|NSIG\rangle=|0111\rangle$ . The photoassociation laser frequency  $\omega_p$  is fixed on the  $|0\frac{1}{2}\frac{3}{2}1\rangle^+ \rightarrow |1111\rangle$  resonance, while a second laser of frequency  $\omega_B$  is tuned over the  $|1111\rangle \rightarrow |0111\rangle$  transition. The baseline fluorescence level is determined by the intensity of  $\omega_p$ , which is less than that used in (a).

quantum numbers. The total molecular spin is  $\vec{G}=\vec{S}+\vec{I}$ . The symmetry of the molecular state with respect to nuclear exchange restricts the possible values of total nuclear spin to  $I=1$  for  ${}^6\text{Li}_2$  [10]. The upper part of the energy diagram in Fig. 1 shows the possible intermediate molecular states that can be accessed from the initial state. The photoassociation process involves an electric dipole transition that couples only to the spatial part of the molecular wave function leading to the total spin selection rule  $\Delta G=0$  and the rotational angular-momentum selection rule  $\Delta N=\pm 1$ .

The final step is to drive the bound-bound transition between the excited intermediate level and the final  $v=9$ ,  $N=0$  level in the  $a^3\Sigma_u^+$  state. Again,  $N$ ,  $S$ ,  $I$ , and  $G$  are good quantum numbers and only  $\Delta G=\Delta S=\Delta I=0$  and  $\Delta N=\pm 1$  transitions are allowed. The dominant hyperfine interaction is given by  $b\vec{S}\cdot\vec{I}$ , where  $b$  is determined by the Fermi-contact interaction [10]. Given that  $N=0$ , the energy

shift relative to the hyperfine center of gravity is

$$E_{NSIG} = \frac{b}{2} [G(G+1) - S(S+1) - I(I+1)]. \quad (2)$$

The energy-level diagram of the final state is shown in the lower right of Fig. 1.

Figure 2(a) shows the one-photon photoassociation spectrum of transitions between initial free states and the excited molecular state. The transitions between specific hyperfine levels are labeled according to the notation of Fig. 1. For the two-photon measurement, the photoassociation laser  $\omega_P$  is tuned to the  $|0\frac{1}{2}\frac{3}{2}1\rangle^+ \rightarrow |1111\rangle$  transition (Fig. 1) and locked at the point of maximum photoassociation signal, while the bound-bound laser frequency  $\omega_B$  is tuned to near resonance between the intermediate state and the bound ground state. Figure 2(b) shows the trap laser-induced fluorescence as a function of the difference frequency  $\Delta\omega = \omega_B - \omega_P$ . The observed resonance corresponds to the  $N=0$ ,  $G=1$  ground state. The  $N=2$  state is also accessible, but is separated from the  $N=0$  state by the rotational splitting of  $\sim 6$  GHz, which places it far from the region shown in Fig. 2 and was not observed. The difference frequency  $\Delta\omega$  is measured with an optical spectrum analyzer, as described in Refs. [7] and [8]. A weighted average of three high-resolution measurements gives  $\Delta\omega = 24.43 \pm 0.02$  GHz. The line shape is a convolution of the free-state energy distribution and the natural linewidth [12]. The uncertainty in  $\Delta\omega$  reflects the uncertainty in the location of the two-photon resonance within the broadened line shape, and the  $\pm 15$ -MHz uncertainty in the calibration of the 1.5-GHz free spectral range of the spectrum analyzer. As a check, the  $v=60$  intermediate state was used instead of  $v=59$  and a consistent value for  $\Delta\omega$  was found.

To determine  $a_T$ , the binding energy of the  $v=9$  level in the absence of hyperfine structure was determined using a first-order perturbation-theory calculation of the hyperfine energy [10]. The  $a^3\Sigma_u^+$  hyperfine-interaction coefficient was calculated to be  $b = a_{2s}/2$ , giving a hyperfine energy of  $-a_{2s}/2$  for the  $|0111\rangle$  state (Fig. 1). In this approximation, the part of the hyperfine Hamiltonian that mixes singlet and triplet levels is ignored. This mixing term is expected to be small when the energy spacing between adjacent singlet and triplet levels is large relative to  $a_{2s}$  [13]. For  ${}^6\text{Li}$ ,  $a_{2s} = 152$  MHz, while the nearest  ${}^6\text{Li}_2$  singlet levels to the  $v=9$  triplet level are the  $v=37$  ( $E_b = 53.5$  GHz) and the  $v=38$  ( $E_b = 1.4$  GHz), and so the approximation is well justified. Since the hyperfine energies of the initial and final states are equivalent, the  $v=9$  binding energy in the absence of hyperfine structure is precisely the measured difference frequency,  $\Delta\omega$ .

Using the measured binding energy, an interaction potential  $V(R)$  may be constructed from which  $a_T$  can be determined with high precision. The basis for  $V(R)$  is the dense Rydberg-Klein-Rees (RKR) values of Zemke and Stwalley [14]. The long-range part, beyond the RKR region, is accurately described by the dispersion coefficients of Ref. [11] and the exchange interaction given in Ref. [15]. The RKR region is referenced to the long-range part through the dissociation energy  $D_e$ . These two regions were smoothly joined using a cubic spline fit. For small  $R$  between  $3a_0$  and  $6a_0$ , the *ab initio* values of Ref. [16] labeled ‘‘OVC’’ were

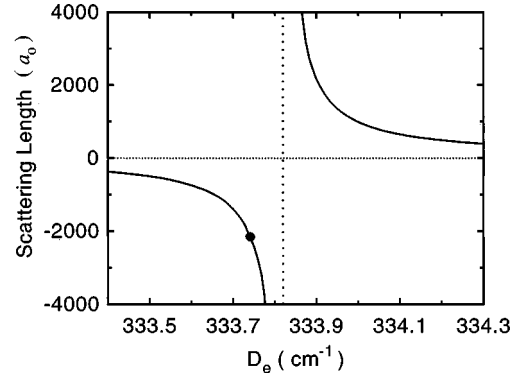


FIG. 3. The triplet scattering length of  ${}^6\text{Li}$  as a function of the dissociation energy  $D_e$  of the  $a^3\Sigma_u^+$  potential using the ‘‘OVC’’ *ab initio* values of Ref. [16] for the inner wall. The solid dot indicates the value of  $D_e$  that yields the measured binding energy for  $v=9$ . As illustrated,  $a_T$  is very sensitive to  $D_e$  for a given inner wall, but we find that  $a_T$  is relatively insensitive to the different combinations of inner wall and  $D_e$  that reproduce the measured binding energy.

used. The OVC values have a positive second derivative that is preferred on physical grounds to the extrapolation of Zemke and Stwalley or the other *ab initio* calculations given in Refs. [16] and [17] which have negative second derivatives.  $D_e$  was adjusted to fit the  $v=9$  eigenvalue of  $V(R)$  to the measured value and was found to be  $333.74 \pm 0.01$   $\text{cm}^{-1}$ . Using one of the other inner wall potentials, instead, results in a shift of the fitted  $D_e$  value by up to  $0.2$   $\text{cm}^{-1}$ . Taking into account all possible combinations of inner walls and dissociation energies that reproduce the measured binding energy, as well as the measurement uncertainty, the triplet scattering length for  ${}^6\text{Li}$  is found to be  $a_T = (-2160 \pm 250)a_0$ .

The triplet scattering length for  ${}^6\text{Li}$  is enormous in magnitude, being the largest known for any atomic system. This indicates a virtual state or near-threshold resonance lying just above the zero-energy limit. As shown in Fig. 3, if the potential were made deeper by just  $0.08$   $\text{cm}^{-1}$ , the virtual state would become bound and the scattering length would change sign.

The experiment reported here is the final in a series of photoassociative spectroscopic measurements made to determine the scattering lengths of lithium. The previous measurements have been reanalyzed in order to increase the precision using the recently improved long-range dispersion coefficients [11]. The new values, although more precise, are consistent with those previously reported by us. In reanalyzing the two-photon data for  ${}^7\text{Li}_2$  using the same procedure outlined for  ${}^6\text{Li}_2$ , the revised  $D_e$  for the  ${}^7\text{Li}_2$   $a^3\Sigma_u^+$  potential is found to be  $333.78 \pm 0.02$   $\text{cm}^{-1}$  with a systematic uncertainty of  $\pm 0.2$   $\text{cm}^{-1}$ . The revised triplet scattering

TABLE I. Singlet and triplet scattering lengths in units of  $a_0$  for isotopically pure and mixed gases of lithium.

	${}^6\text{Li}$	${}^7\text{Li}$	${}^6\text{Li}/{}^7\text{Li}$
$a_T$	$-2160 \pm 250$	$-27.6 \pm 0.5$	$40.9 \pm 0.2$
$a_S$	$45.5 \pm 2.5$	$33 \pm 2$	$-20 \pm 10$

length for  ${}^7\text{Li}$  is  $a_T = (-27.6 \pm 0.5)a_0$ . For the  ${}^6\text{Li}{}^7\text{Li}$  triplet, the average value of  $D_e = 333.76 \pm 0.02 \text{ cm}^{-1}$  yields  $a_T = (40.9 \pm 0.2)a_0$ .

The singlet scattering lengths were originally found by fitting to a minimum observed in the one-photon photoassociation singlet spectrum [9]. A coupled-channel calculation to account for singlet-triplet mixing [18] has been used to reanalyze these data. The singlet potential used in the coupled-channel calculation is that described in Ref. [15], modified by the improved long-range coefficients. For the case of  ${}^6\text{Li}_2$ , the  $D_e$  of the  $X^1\Sigma_g^+$  state is found to be  $8516.70 \pm 0.10 \text{ cm}^{-1}$  with a scattering length  $a_S = (45.5 \pm 2.5)a_0$ . For  ${}^7\text{Li}_2$ , the  $D_e$  is found to be  $8516.75 \pm 0.10 \text{ cm}^{-1}$  with a scattering length of  $a_S = (33 \pm 2)a_0$ . The reported uncertainty is at the limit of the experimental precision. For the  ${}^6\text{Li}{}^7\text{Li}$  singlet, an average value of  $D_e = 8516.73 \pm 0.10 \text{ cm}^{-1}$  is used to obtain

$a_S = (-20 \pm 10)a_0$ . These results are summarized in Table I. These scattering lengths and corresponding potentials can be used to determine the low-energy scattering length of any binary collision in lithium. Some experimentally interesting collisional channels have been analyzed using a coupled-channel approach [19].

The authors are grateful to H. Stoof for help with the coupled-channel calculations and to C. Sackett for discussions. The work at Rice is supported by the National Science Foundation, the Welch Foundation, and NASA. W.I.M. received support from the Fannie and John Hertz Foundation. A.D. acknowledges the support of the Division of Chemical Sciences, Office of Basic Energy Sciences, Office of Energy Research, U.S. Department of Energy. R.C. is supported by the National Science Foundation through the Institute for Theoretical Atomic and Molecular Physics (ITAMP).

- 
- [1] M. H. Anderson *et al.*, *Science* **269**, 198 (1995); C. C. Bradley *et al.*, *Phys. Rev. Lett.* **75**, 1687 (1995); K. B. Davis *et al.*, *ibid.* **75**, 3969 (1995).
- [2] Cf. K. Huang, *Statistical Mechanics*, 2nd ed. (John Wiley & Sons, New York, 1987).
- [3] H. T. C. Stoof, *Phys. Rev. A* **49**, 3824 (1994).
- [4] P. A. Ruprecht, M. J. Holland, K. Burnett, and M. Edwards, *Phys. Rev. A* **51**, 4704 (1995); Y. Kagan, G. V. Shlyapnikov, and J. T. M. Walraven, *Phys. Rev. Lett.* **76**, 2670 (1996); M. Houbiers and H. T. C. Stoof, *Phys. Rev. A* **54**, 5055 (1996); H. T. C. Stoof, *J. Stat. Phys.* (to be published).
- [5] C. C. Bradley, C. A. Sackett, and R. G. Hulet, *Phys. Rev. Lett.* **78**, 985 (1997).
- [6] H. T. C. Stoof, M. Houbiers, C. A. Sackett, and R. G. Hulet, *Phys. Rev. Lett.* **76**, 10 (1996).
- [7] E. R. I. Abraham, W. I. McAlexander, C. A. Sackett, and R. G. Hulet, *Phys. Rev. Lett.* **74**, 1315 (1995).
- [8] E. R. I. Abraham, N. W. M. Ritchie, W. I. McAlexander, and R. G. Hulet, *J. Chem. Phys.* **103**, 7773 (1995).
- [9] R. Côte, A. Dalgarno, Y. Sun, and R. G. Hulet, *Phys. Rev. Lett.* **74**, 3581 (1995); E. R. I. Abraham *et al.*, *Phys. Rev. A* **53**, R3713 (1996).
- [10] E. R. I. Abraham, W. I. McAlexander, H. T. C. Stoof, and R. G. Hulet, *Phys. Rev. A* **53**, 3092 (1996).
- [11] Z.-C. Yan, J. F. Babb, A. Dalgarno, and G. W. F. Drake, *Phys. Rev. A* **54**, 2824 (1996).
- [12] J. L. Bohn and P. S. Julienne, *Phys. Rev. A* **54**, R4637 (1996).
- [13] A. J. Moerdijk and B. J. Verhaar, *Phys. Rev. A* **51**, R4333 (1995).
- [14] W. T. Zemke and W. C. Stwalley, *J. Phys. Chem.* **97**, 2053 (1993).
- [15] R. Côte, A. Dalgarno, and M. J. Jamieson, *Phys. Rev. A* **50**, 399 (1994).
- [16] D. D. Konowalow, R. M. Regan, and M. E. Rosenkrantz, *J. Chem. Phys.* **81**, 4534 (1984).
- [17] I. Schmidt-Mink, W. Müller, and W. Meyer, *Chem. Phys.* **92**, 263 (1985).
- [18] H. T. C. Stoof, J. M. V. A. Koelman, and B. J. Verhaar, *Phys. Rev. B* **38**, 4688 (1988).
- [19] F. A. van Abeelan, B. J. Verhaar, and A. J. Moerdijk (unpublished).